Journal of Mammalian Evolution (2023) 30:907–922
https://doi.org/10.1007/s10914-023-09689-x

RESEARCH

Endocranial cast anatomy of the Early Miocene glyptodont *Propalaehoplophorus australis* (Mammalia, Xenarthra, Cingulata) and its evolutionary implications

Adrian Troyelli[1,2,3,4] · Guillermo Hernán Cassini[1,2,3,4] · German Tirao[4,5] · Alberto Boscaini[4,6] · Juan Carlos Fernicola[1,2,4,7]

Accepted: 29 September 2023 / Published online: 10 November 2023

Abstract

Propalaehoplophorus is an Early Miocene genus of glyptodonts, a group of extinct armored mammals closely related to armadillos and endemic to South America. Here, we present the first digital reconstruction of the endocranial cavity of the glyptodont *Propalaehoplophorus australis* and compare it to endocasts of Late Miocene and Pleistocene glyptodonts, pampatheres, and extant armadillos. *Propalaehoplophorus australis* shares exclusively with other glyptodonts the neocortical sulcation pattern and cranial nerve (CN) V_3 pathway. It also shares with both other glyptodonts and pampatheres the rhinal fissure trajectory, small piriform lobe, marked dorsal expansion of neocortical fronto-parietal region, conspicuous thickness of superior longitudinal sinus, and presence of a well-marked lateral sulcus and medial shape of petrosal bone; this last trait is also observable in *Chlamyphorus*. The olfactory bulbs of *Pr. australis, Holmesina,* and *Pampatherium* are anteriorly elongated and partially laterally divergent as in the glyptodont *Pseudoplohophorus absolutus*. Other features, like the globular proximal shape of olfactory peduncles, topological arrangement of CNs IX-XII, differentiated petrosal lobule of paraflocculus, and orientation of spinal cord are shared among *Pr. australis, Ps. absolutus*, pampatheres, and extant armadillos. The similarities between *Pr. australis*, remaining glyptodonts, and pampatheres could be synapomorphies of pampatheres + glyptodonts. By contrast, *Pr. australis*, pampatheres, and all the analyzed armadillos share the same configuration of the pathway of CNs IX-XII, a feature that could support the basal position of *Pr. australis* among glyptodonts for which cranial remains are known. In this context, the brain cavity seems to be a promising source of information for revealing the evolutionary history of this mammalian clade.

Keywords Cingulata · Endocast · Glyptodonts · Neuroanatomy · Phylogeny

✉ Adrian Troyelli
atroyelli@unlu.edu.ar

[1] Departamento de Ciencias Básicas, Universidad Nacional de Luján (UNLu), Ruta Nacional 5 y Av. Constitución, 6700 Luján, Buenos Aires, Argentina

[2] Laboratorio de Anatomía y Biología Evolutiva de Vertebrados (LABEV), Universidad Nacional de Luján (UNLu), Ruta Nacional 5 y Av. Constitución, 6700 Luján, Buenos Aires, Argentina

[3] División Mastozoología, Museo Argentino de Ciencias Naturales "Bernardino Rivadavia" (MACN-BR), Av. Ángel Gallardo 470, C1405DJR Ciudad Autónoma de Buenos Aires, Argentina

[4] Consejo Nacional de Investigaciones Científicas y Técnicas (CONICET), Buenos Aires, Argentina

[5] IFEG CONICET Facultad de Matemática, Astronomía, Física y Computación, Universidad Nacional de Córdoba, Haya de La Torre y Medina Allende, X5000HUA Córdoba, Argentina

[6] Instituto de Ecología, Genética y Evolución de Buenos Aires (IEGEBA – CONICET), Departamento de Ecología, Genética y Evolución, Facultad de Ciencias Exactas y Naturales, Universidad de Buenos Aires. Int. Güiraldes, 2160, C1428EGA Ciudad Autónoma de Buenos Aires, Argentina

[7] División Paleontología Vertebrados, Museo Argentino de Ciencias Naturales "Bernardino Rivadavia" (MACN-BR), Av. Ángel Gallardo 470, C1405DJR Ciudad Autónoma de Buenos Aires, Argentina

Introduction

Cingulata (armadillos, glyptodonts, pampatheres, and peltephilids), together with Pilosa (sloths and anteaters), constitute Xenarthra, a monophyletic group and one of the four major clades of placental mammals that originated and initially radiated in South America (Engelmann 1985; Delsuc et al. 2003; Gaudin and Mcdonald 2008; O'Leary et al. 2013; Gaudin and Croft 2015; Gibb et al. 2016; Padberg 2017; Prothero 2017; Quiñones et al. 2019). Within Cingulata, Glyptodontia (sensu Fernicola 2008), with more than 60 recognized species, represents one of the most speciose groups (McKenna and Bell 1997). Glyptodonts range chronologically from the Late Eocene to the Early Holocene (Zurita et al. 2016a, b; Fernicola et al. 2021) and are last recovered at the end of the Last Glacial Period, around 10,000 years ago, during the megafaunal extinction (Barnosky et al. 2016; Delsuc et al. 2016; Prates and Perez 2021).

Glyptodonts are usually considered as herbivores displaying morphologies that are indicative of selective or bulk feeding strategies in closed or open environments, and pampatheres show variation related to oral processing of coarse vegetation (Vizcaíno et al. 1998, 2004, 2006, 2011b, 2012; De Iuliis et al. 2001; Vizcaíno 2009). On the other hand, extant armadillos show additional feeding behaviors such as insectivory (with strict myrmecophagy) to omnivory (including small vertebrates, plant material, and carrion) (Abba et al. 2011, 2015; Wallace and Painter 2013; Gallo et al. 2019). The body mass of extant armadillos ranges from micromammals (i.e., less than 1 kg), such as the pink fairy armadillo (*Chlamyphorus* ~ 120 g; Superina 2011), to medium size forms (i.e., 10–100 kg; sensu Cassini et al. 2012), such as the giant armadillo (*Priodontes* ~ 30 kg; Carter et al. 2016). By contrast, many extinct cingulates exceed this range, with pampatheres usually exceeding 100 kg (i.e., large-sized 100–1,000 kg sensu Cassini et al. 2012), and glyptodonts having body masses ranging from ~ 70 kg to 1,000 + kg (in *Asterostemma* and *Doedicurus*, respectively) (Vizcaíno et al. 2006, 2011a, b; Tambusso and Fariña 2015b), with the largest members qualifying as strict megamammals (sensu Owen-Smith 1988; i.e., ≥ 1,000 kg).

Glyptodonts have remarkable morphological features such as a carapace formed only by immovable osteoderms, fused thoracic and lumbar vertebrae, columnar hind-limbs, tall and anteroposteriorly short skull with rostrum and masticatory apparatus placed ventral to the braincase, a conspicuous descending zygomatic process, and high-crowned and ever-growing cheek teeth (i.e., hypselodont) (Huxley 1865; Gillette and Ray 1981; Fariña and Vizcaíno 2001; Fernicola 2008; Vizcaíno 2009; Vizcaíno et al. 2011a, b; Fernicola and Porpino 2012; Fernicola et al. 2012; Machado et al. 2022).

Since the first phylogenetic hypotheses of xenarthrans based on morphological data of Engelmann (1985), glyptodonts have been recognized as a well-supported monophyletic group. However, the phylogenetic position of glyptodonts among Cingulata is controversial. Engelmann (1985) suggested a basal dichotomy between extant and extinct armadillos on one side and pampatheres, glyptodonts, and the armadillos *Eutatus* and *Proeutatus* on the other. The association of glyptodonts, pampatheres, and *Proeutatus* has been validated by subsequent cladistic analyses but with *Eutatus* occupying a more basal position within cingulates (Gaudin and Wible 2006; Billet et al. 2011; Herrera et al. 2017). However, the recent incorporation of ancient DNA from the glyptodont *Doedicurus* has revealed a novel phylogenetic scheme, where glyptodonts are the sister group of a clade that includes chlamyphorine and tolypeutine armadillos (Delsuc et al. 2016; Mitchell et al. 2016). Mitchell et al. (2016) reanalyzed the morphological data matrix of Billet et al. (2011) with a molecular phylogenetic constraint and found support for a sister-group relationship between *Proeutatus* and the clade *Propalaehoplophorus* + *Vassallia*, with that clade positioned as sister to *Eutatus* + *Chlamyphorus*.

Among glyptodonts, there is a general consensus on the basal position of medium-sized (74–115 kg; Vizcaíno et al. 2011a) Early Miocene *Propalaehoplophorus* (Fernicola 2008; Porpino et al. 2010, 2014; Fernicola and Porpino 2012; Fernicola et al. 2018). In addition, these authors found support for a basal dichotomy between the clades Propalaehoplophorinae/dae and Glyptodontoinei (sensu Fernicola 2008; i.e., all the remaining glyptodonts) using parsimony-based analyses on different character subsets (e.g., craniodental, postcranial and/or exoskeletal data) (see also Croft et al. 2007 for an alternative phylogenetic arrangement). However, recent phylogenetic analyses do not support the Propalaehoplophorinae/dae and Glyptodontoinei monophyly (Zurita et al. 2013a, b, 2016a, b; Cuadrelli et al. 2020; Barasoain et al. 2022), although the discrepancies could be due to the different selections of taxa and characters in the distinct datasets respect to previous studies.

The neuroanatomy and neuromorphology of cingulates have been explored through endocasts, both natural and reconstructed using plaster-silicone, since the end of the XIX century (Gervais 1869; Dechaseaux 1958, 1962; Dozo 1987, 1989, 1994, 1998). The first description of a *Propalaehoplophorus* endocast was performed by Dozo (1989) through observation of a natural endocast. However, its detailed analysis was impossible due to preservational issues, preventing observation of the olfactory bulbs, the cerebellar region, and the cranial nerve pathways. Nowadays, computed tomography (CT) permits exploring and digitally reconstructing the internal cranial anatomy through non-invasive methods. This procedure has been revolutionary for extinct and

extant mammalian neuroanatomy, providing novel phylogenetic, functional, and paleobiological information (Macrini 2006; Macrini et al. 2007a, b; Witmer and Ridgely 2008; Orliac et al. 2012; Ahrens 2014; Dozo and Martínez 2016; Orliac and O'Leary 2016; Bertrand et al. 2019, 2021, 2023; Fernández-Monescillo et al. 2019; Martínez et al. 2019; Perini et al. 2022). Recently, digital reconstructions of xenarthran endocranial structures like those of the ground sloths *Catonix* and *Glossotherium* have been compared to their homologues in extant relatives (Boscaini et al. 2020a, b). Other authors have studied an extensive sample of bony labyrinth casts in fossil and living xenarthrans (Billet et al. 2015). Among cingulates, (Tambusso and Fariña 2015a, b; Tambusso et al. 2023) comparatively described the digital endocasts of the glyptodonts *Doedicurus*, *Glyptodon*, *Panochthus,* and *Pseudoplohophorus*, and the pampatheres *Holmesina* and *Pampatherium* to extant long-nosed (i.e., *Dasypus*), and hairy (i.e., *Euphractus*, *Chaetophractus* and *Zaedyus*), and tolypeutine (i.e., *Cabassous, Priodontes* and *Tolypeutes*) armadillos, including a discussion of potential neuroanatomical characters and their phylogenetic and evolutionary implications. Recently, Christen et al. (2023) described cranial and endocranial structures (i.e., endocast, bony labyrinth, and intraosseous canals) in Pleistocene glyptodonts *Doedicurus*, *Glyptodon*, *Panochthus,* and *Neosclerocalyptus*, discussing its phylogenetic value in relation to the recent genealogical arrangement of glyptodonts (Núñez Blasco et al. 2021). In addition, Tambusso et al. (2021, 2023) analyzed the inner ear morphology in phylogenetic and functional contexts, including all genera of extant armadillos (except *Calyptophractus*) and glyptodonts and pampatheres mentioned above, recovering a strong resemblance that is congruent with their relationships as suggested by recent molecular analyses (Delsuc et al. 2016; Mitchell et al. 2016) and some morphology-based studies (Engelmann 1985; Gaudin and Wible 2006; Billet et al. 2011; Herrera et al. 2017; Fernicola et al. 2018). Finally, Le Verger et al. (2021) performed a comparative analysis and explored the evolutionary scenarios using an extensive sample of cingulates, including glyptodonts and extinct and extant armadillos, based on the digital reconstruction of intracranial osseous canals (i.e. nasolacrimal, palatine, sphenopalatine, among others). They found phylogenetic results that are similar to those of Tambusso et al. (2021) concerning the relationships among glyptodonts, pampatheres, and chlamyphorine armadillos. However, internal glyptodont relationships are unresolved in both cases. Considering this context, it is evident that the endocranial anatomy of Cingulata could represent a promising source of data to illuminate their phylogenetic relationships.

The present contribution aims to provide 3D digital reconstructions of the brain cavity, cranial nerves, and vasculature of *Propalaehoplophorus australis* and perform a morphological comparative analysis with other cingulate endocasts (glyptodonts, pampatheres, and extant armadillos), further evaluating their anatomical, phylogenetic, and paleobiological implications.

Materials and methods

Specimens

Our study focused on a specimen of *Propalaehoplophorus australis*, MLP 16–15, which consists of cranium, mandible, and skeleton. It was recovered from the Santa Cruz Formation (latest Early Miocene), Santa Cruz, Argentina, and first figured in Lydekker (1894: p. 3, pl. 32).

The comparative sample comprised 12 species, including five extant armadillos (*Chaetophractus villosus*, *Chlamyphorus truncatus, Dasypus novemcinctus*, *Euphractus sexcinctus,* and *Zaedyus pichiy*), and six extinct cingulates: the glyptodonts *Doedicurus* sp., *Glyptodon* sp., *Panochthus tuberculatus*, *Pseudoplohophorus absolutus*, and the pampatheres *Holmesina cryptae*, *Pampatherium humboldtii,* and *Pampatherium typum*. For a complete list of specimens and sources of anatomical information, see Table 1.

Computed tomographies and digital reconstructions

The skulls of *Doedicurus* sp., *Pampatherium typum*, *Panochthus tuberculatus*, and *Propalaehoplophorus australis* were scanned using the Phillips Vereos PET/CT scanner at CEUNIM/UNSAM Institute, Buenos Aires, Argentina. The scan includes 513 slices with an interslice thickness of 0.67 mm on a 16-bit grayscale. The micro CT data of extant specimens housed at MACN-Ma resulted in a slice number range of 206–642, depending on the specimen, with a slice thickness of 0.194 mm. These CT scans were acquired using non-commercial equipment developed by the "Grupo de Espectroscopía Atómica y Nuclear (GEAN)" at the Facultad de Matemática, Astronomía y Física (FaMAF), Córdoba, Argentina. The micro CT scan of the TMM M specimen *D. novemcinctus* was obtained from the DigiMorph online repository (http://www.digimorph.org/index.phtml) of the University of Texas. The micro CT scans of FMNH M, and MNHN.F.PAM were acquired from the MorphoSource digital online repository (https://www.morphosource.org) of Duke University (Table 1).

The digital reconstructions of the brain endocasts of all specimens (Online Resource 1) were created using digital tools for the semi-automatic segmentation process of the open-source software 3DSlicer (Fedorov et al. 2012). The 3D models of skulls and brain cavities were exported from 3DSlicer as Polygon File Format (PLY) files. Visualization of 3D meshes was carried out using MeshLab (Cignoni et al. 2008).

Table 1 List of specimens included and CT/microCT parameters

Family/Subfamily	Species	Museum collection	Collection number	CT/microCT/3D mesh source	Slice number	Slice thickness (mm)
Euphractinae	*Chaetophractus villosus*	MACN-Ma	27802	GEAN-FaMAF	642	0.194
Chlamyphorinae	*Chlamyphorus truncatus*	MACN-Ma	24.46	GEAN-FaMAF	206	0.194
Chlamyphorinae	*Chlamyphorus truncatus*	FMNH M	39468	University of Chicago – Paleo CT (MorphoSource: ark:/87602/m4/377398)	1746	0.034
Dasypodinae	*Dasypus novemcinctus*	MACN-Ma	50.123	GEAN-FaMAF	550	0.194
Dasypodinae	*Dasypus novemcinctus*	TMM M	7417	University of Texas – Vertebrate Palaeontology Laboratory (DigiMorph)	944	0.037
Doedicurinae	*Doedicurus* sp.	MACN-Pv	2762	CEUNIM-UNSAM	768	0.326
Euphractinae	*Euphractus sexcinctus*	MACN-Ma	49.38	GEAN-FaMAF	639	0.194
Glyptodontinae	*Glyptodon* sp.	MNHN.F.PAM	759	Muséum National d'Histoire Naturelle—Technical Platform (MorphoSource: ark:/87602/m4/M54401)	2226	0.148
Pampatheriidae	*Holmesina cryptae*	LPP PV	002	Tambusso et al. (2023)	-	-
Pampatheriidae	*Pampatherium typum*	MACN-Pv	11543	CEUNIM-UNSAM	646	0.21
Pampatheriidae	*Pampatherium humboldtii*	MHD P	28	Tambusso and Fariña (2015b)	-	-
Panochthinae	*Panochthus tuberculatus*	MLP	16–38	CEUNIM-UNSAM	768	0.326
Propalaehoplophorinae	*Propalaehoplophorus australis*	MLP	16–15	CEUNIM-UNSAM	510	0.134
Glyptodontidae	*Pseudoplohophorus absolutus*	FC DPV	595	Tambusso and Fariña (2015a)	-	-
Euphractinae	*Zaedyus pichiy*	MACN-Ma	30.33	GEAN-FaMAF	375	0.194

Neuroanatomical reference

Endocranial structure identification was mainly based on previous (solid or digital) models of the brain cavity and encephalic dissections in cingulates (e.g., Gervais 1869; Cope 1889; Dechaseaux 1958, 1962; Dozo 1989, 1998; Araújo et al. 2015; Tambusso and Fariña 2015a, b; Le Verger et al. 2021; Christen et al. 2023; Tambusso et al. 2023), as well as other extinct and extant xenarthrans (Dozo 1989; Padberg 2017; Boscaini et al. 2020a, b). In addition, we consulted the literature on other mammalian representatives (Gannon et al. 1988; Macrini 2006; Macrini et al. 2007a, b, 2010; Aurboonyawat et al. 2008; Treuting et al. 2017; De Iuliis and Pulerá 2019). Particularly in glyptodonts, the last teeth were taken as a reference to horizontalize the cranium due to the sigmoid shape of the palatal process of the maxilla (Fernicola 2008). To standardize descriptions and comparisons, the skulls were positioned in lateral view, with the palate oriented horizontally, illustrating the relative position of the endocast through the bony transparency of the skull (Fig. 1b–f). For the phylogenetic inferences, we assembled an ad hoc topology of only the taxa included in the analysis based on previous analyses (i.e., Delsuc et al. 2016; Mitchell et al. 2016; Fernicola et al. 2018) that includes only taxa discussed in the present contribution (Fig. 2).

Institutional abbreviations FMNH M: Field Museum Natural History, Extant Mammal Collection, Chicago, USA; MACN-Ma: Museo Argentino de Ciencias Naturales "Bernardino Rivadavia", Colección Nacional de Mastozoología, Ciudad Autónoma de Buenos Aires, Argentina; MACN-Pv: Museo

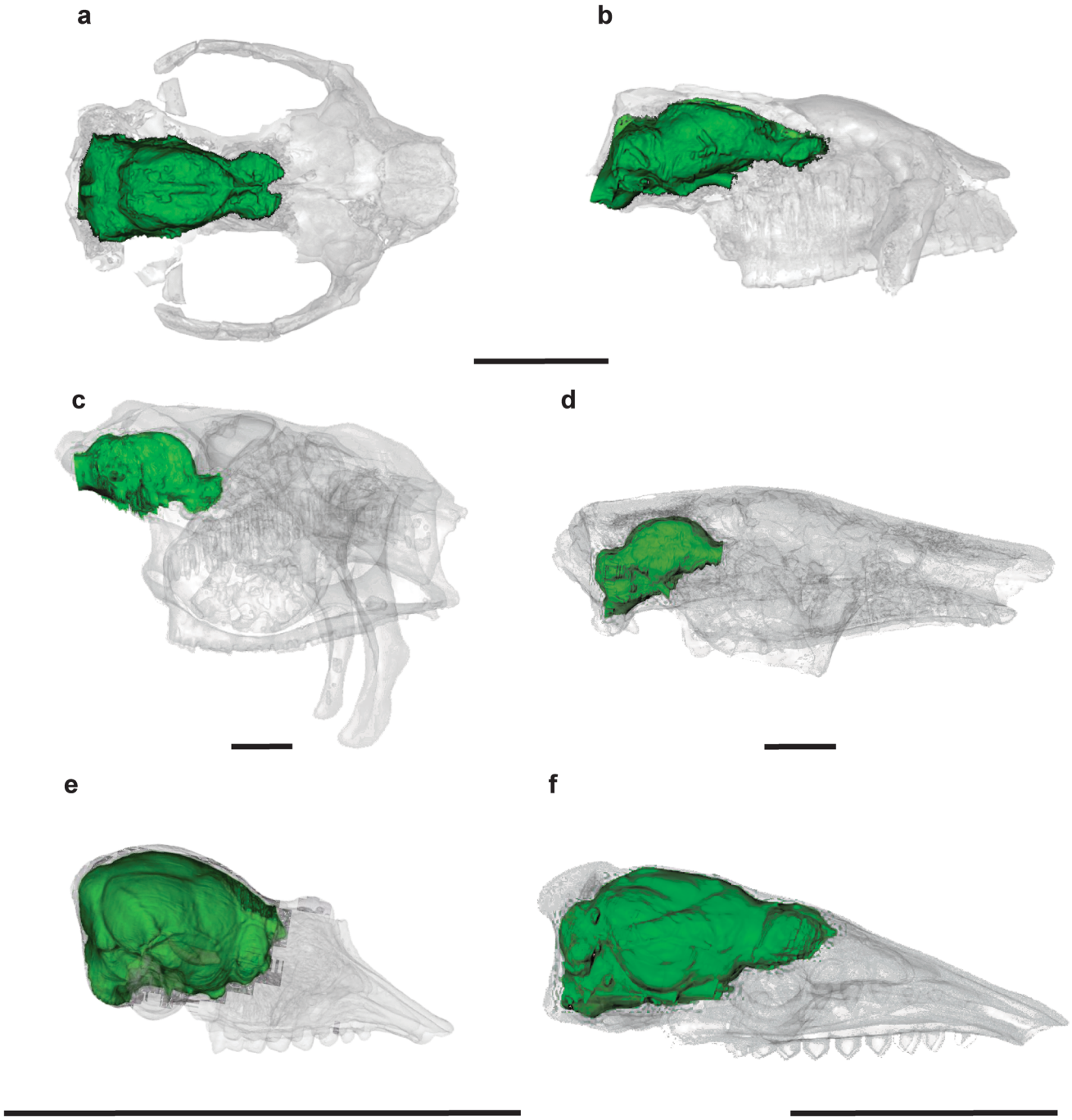

Fig. 1 Endocranial cavity (green) and comparative relative position in a transparent cranium (grey). **a-b.** *Propalaehoplophorus australis* (MLP 16–15) in dorsal (**a**) and right lateral (**b**) views; **c-f**. right lateral views of: **c**. *Glyptodon* sp. (MNHN.F.PAM 759); **d**. *Pampatherium typum* (MACN-Pv 11543); **e**. *Chlamyphorus truncatus* (MACN-Ma 24.46); **f**. *Chaetophractus villosus* (MACN-Ma 27802). Scale bars equal 50 mm

Argentino de Ciencias Naturales "Bernardino Rivadavia", Colección Nacional de Paleovertebrados, Ciudad Autónoma de Buenos Aires, Argentina; MLP: Museo de La Plata, La Plata, Argentina; MNHN.F.PAM: Muséum National d'Histoire Naturelle, Zoologie et Anatomie comparée collections, fossil mammal collections, Pampean, Paris, France; TMM M: Mammal Collections of the Vertebrate Paleontology Laboratory, Texas Memorial Museum, Austin, Texas, USA.

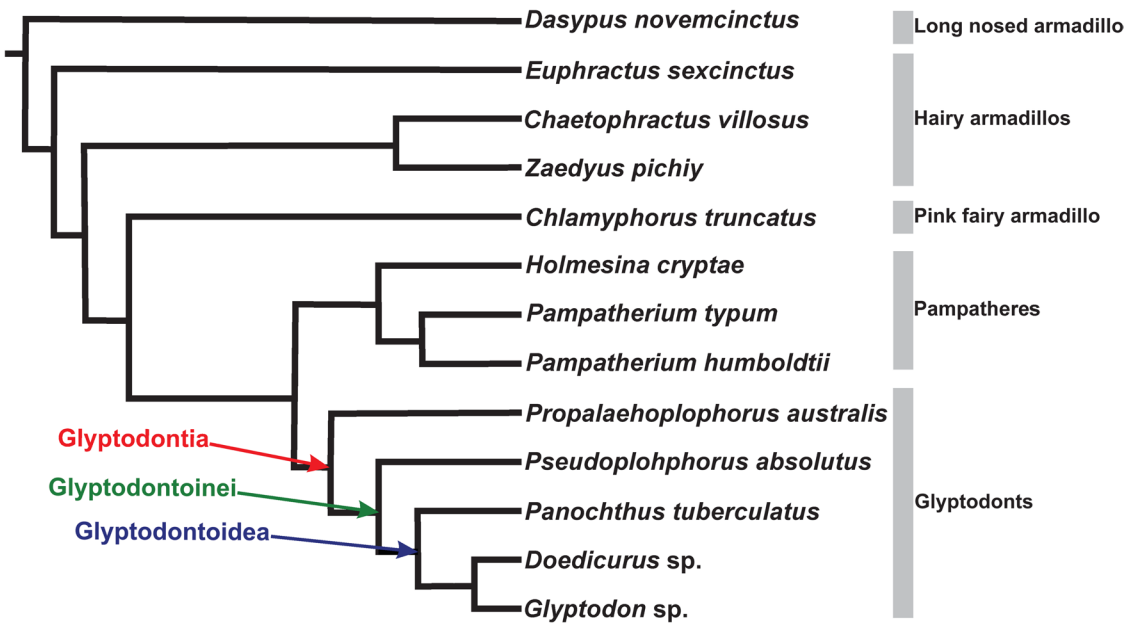

Fig. 2 Phylogenetic tree of the analyzed cingulate taxa based on Delsuc et al. (2016), Mitchell et al. (2016), and Fernicola et al. (2018)

Results

Forebrain

The anteriormost telencephalon of *Propalaehoplophorus australis* displays olfactory bulbs elongated anteroposteriorly with convex lateral edges. This shape is similar to that of *Holmesina* and *Pampatherium*, although in this latter taxon, the olfactory bulbs are thinner mediolaterally (Figs. 3a, b and 5d; Tambusso et al. 2023: fig. 4a, b). The condition of *Pr. australis* in showing a partial dorsal divergence of the olfactory bulbs is similar to *Pseudoplohophorus* and *Pampatherium*. By contrast, extant armadillos display olfactory bulbs that are non-divergent or divergent only in their anteriormost end (Figs. 3, 4, 5 and 6; Tambusso and Fariña 2015b: fig. 2), whereas in Pleistocene glyptodonts, the olfactory bulbs are completely separated (Fig. 4). Additionally, in *Pr. australis* and *Ps. absolutus* the sinus longitudinal superior is anteriorly extended, reaching the half length of olfactory bulbs on their dorsal surface (Fig. 3; Tambusso and Fariña, 2015a: fig. 2). In armadillos and pampatheres, this vessel extends anteriorly, reaching the circular fissure (Fig. 6; Tambusso et al. 2023: fig. 4a, b). In Pleistocene glyptodonts, the sinus longitudinal superior does not extend beyond the anteriormost extreme of cerebral hemispheres (Fig. 4). In *Propalaehoplophorus*, the olfactory bulbs are ventrally oriented in relation to the cerebral hemispheres (Fig. 3b), as observed in Glyptodontei (all remaining glyptodonts included) and pampatheres (Figs. 4 and 5). In ventral view, immediately posterior to the olfactory bulbs, the olfactory peduncles are tubular anteriorly, enlarging and displaying a globular shape posteriorly (Fig. 3c). This last trait is present in all the analyzed cingulates, except for Pleistocene glyptodonts, which display flat ventral surfaces of the olfactory peduncles (Fig. 4). The piriform lobe of *Propalaehoplophorus* shows a relatively small size in the lateral exposure of the telencephalon as in pampatheres and glyptodonts. In contrast, in armadillos, the piriform lobe occupies almost all the lateral side of the telencephalon (Figs. 3, 4, 5 and 6; Tambusso et al. 2023: fig. 4a, b). The piriform lobe is laterodorsally flanked by a distinguishable orbito-temporal canal in all cingulates. This canal housed the rhinal caudal vein that derived from the lateral branching of the transverse sinus (Figs. 3, 4, 5 and 6).

The posteriormost telencephalon of *Pr. australis* displays ovoid shape of cerebral hemispheres, reaching their maximum mediolateral expansion at the level of the temporal lobes dorsally. This feature is similar to *Ps. absolutus* and extant armadillos, with the exclusion of *Chlamyphorus*, which shows a quadrangular shape of the telencephalon as in Pleistocene glyptodonts and pampatheres (Figs. 4, 5 and 6). The neocortical anterior region (i.e., frontal and parietal lobes) is dorsally extended in lateral view. The neocortex is separated dorsoventrally from the paleocortex (i.e., olfactory structures) by an anteroposteriorly continuous rhinal fissure (Fig. 3b), as well as in remaining glyptodonts and pampatheres (Figs. 4 and 5). In armadillos, the anterior neocortical region is flatter in lateral view, and the rhinal fissure is discontinuous, showing two distinct branches (anterior and posterior). The neocortical arrangement of *Pr. australis* shows undifferentiated frontal and parietal lobes occupying most of the neocortical surface. However, two well-defined

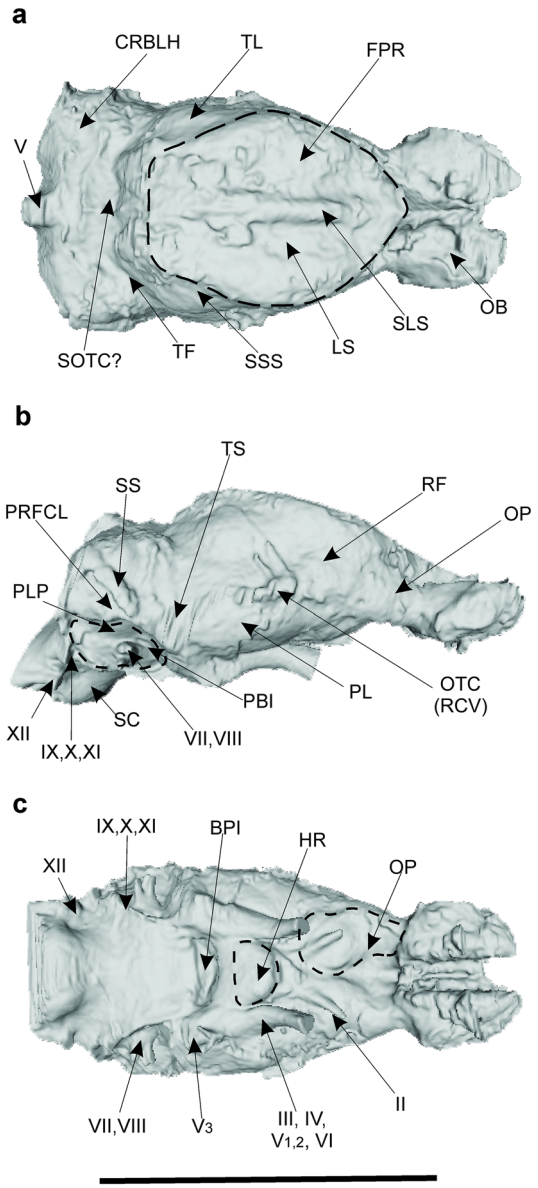

Fig. 3 Endocast of *Pr. australis* (MLP 16–15) in dorsal (**a**), right lateral (**b**), and ventral (**c**) views. Abbreviations: **BPI**, basilar process imprint; **CRBLH**, cerebellar hemispheres; **FPR**, frontoparietal region; **HR**, hypophyseal region; **LS**, lateral sulcus; **OB**, olfactory bulbs; **OP**, olfactory peduncules; **OTC**, orbito temporal canal; **PBI**, petrosal bone imprint; **PL**, piriform lobe; **PLP**, petrosal lobe of paraflocculus; **PRFCL**, parafocculus; **RCV**, rhinal caudal vein; **RF**, rhinal fissure; **SC**, spinal cord; **SLS**, superior longitudinal sinus; **SOTC**, sulci of ossified tentorium cerebelli; **SSS**, suprasylvian sulcus; **TF**, transverse fissure; **TL**, temporal lobe; **TS**, transverse sinus; **SS**, sigmoid sinus; Cranial nerves are indicated by roman numbers (II-XII). Scale bar equals 50 mm

sulci are observable in the neocortex: the lateral sulcus, whose pathway is parallel to the middle line dividing the cerebral hemispheres, and the suprasylvian sulcus that ascends obliquely from the rhinal fissure, delimiting the temporal lobes dorsally (Fig. 3a). The presence of undivided frontoparietal lobes and these neocortical sulci is observable in all glyptodonts. Pampatheres exhibit these sulci as well, but frontal and parietal lobes are delimited anteroposteriorly by the presylvian sulcus (Fig. 5a; Tambusso et al. 2023: fig. 4a, b). Armadillos show a neocortical sulcation similar to that of pampatheres, except for the absence of the lateral sulcus (Fig. 6). At the middle line of the neocortex, the cast of the superior longitudinal sinus is well-marked in *Pr. australis* like in the remaining glyptodonts and pampatheres, and unlike armadillos, that display a minor or null development of this sinus. However, *Chlamyphorus* shows a distinguished relative size of this vessel (Figs. 3, 4, 5 and 6).

In *Pr. australis*, the diencephalon is represented only by the hypophyseal region that shows a trapezoidal shape, being slightly wider mediolaterally than anteroposteriorly (Fig. 3c). It is also narrower anteriorly, in the proximity of the optic chiasm, than posteriorly. The shape of the hypophyseal region is similar among glyptodonts, pampatheres, and hairy armadillos and different from the long-nosed armadillo, which display a less detached hypophyseal region. The pink fairy armadillo shows a large-sized hypophysis that is oval shaped (mediolaterally wider than anteroposteriorly longer) in ventral view (Figs. 3, 4, 5 and 6). In *Pr. australis*, posterior to the hypophyseal region, a deep depression is observable, corresponding to the basilar process of the basioccipital that protrudes into the endocranial cavity (Fig. 3c). This feature is evident in glyptodonts and pampatheres, but indistinguishable in all the analyzed armadillos (Figs. 4, 5 and 6; Tambusso et al. 2023: fig. 4a, b).

Hindbrain

The cerebellum is separated from the telencephalon at the level of the transverse fissure dorsally and the root of the mandibular branch of the trigeminal nerve ventrally. In all the observed armadillos, a detached tentorium cerebelli is observable in the roof of the brain cavity. This structure is placed medially, orthogonal to the longitudinal fissure, and roughly mediolaterally wide as the vermis. In all the analyzed armadillos the ossified tentorium cerebelli leaves a deep sulcus on the dorsal surface of the endocast, right at the separation between the cerebral hemispheres and the cerebellum (Fig. 6). In the pampatheres *Pampatherium* and *Holmesina*, a detached sulcus of the ossified tentorium cerebelli was detected (Fig. 5a; Tambusso et al. 2023: fig: 4a, b) but it is apparently lacking in *Pseudoplohophorus* and completely absent in Pleistocene glyptodonts (Fig. 4). An intermediate condition, however, is observed in *Propalaehoplophorus,* in which a "w-shaped" sulcus is detectable right at the separation between telencephalon and rhombencephalon (Fig. 3a). This sulcus could represent

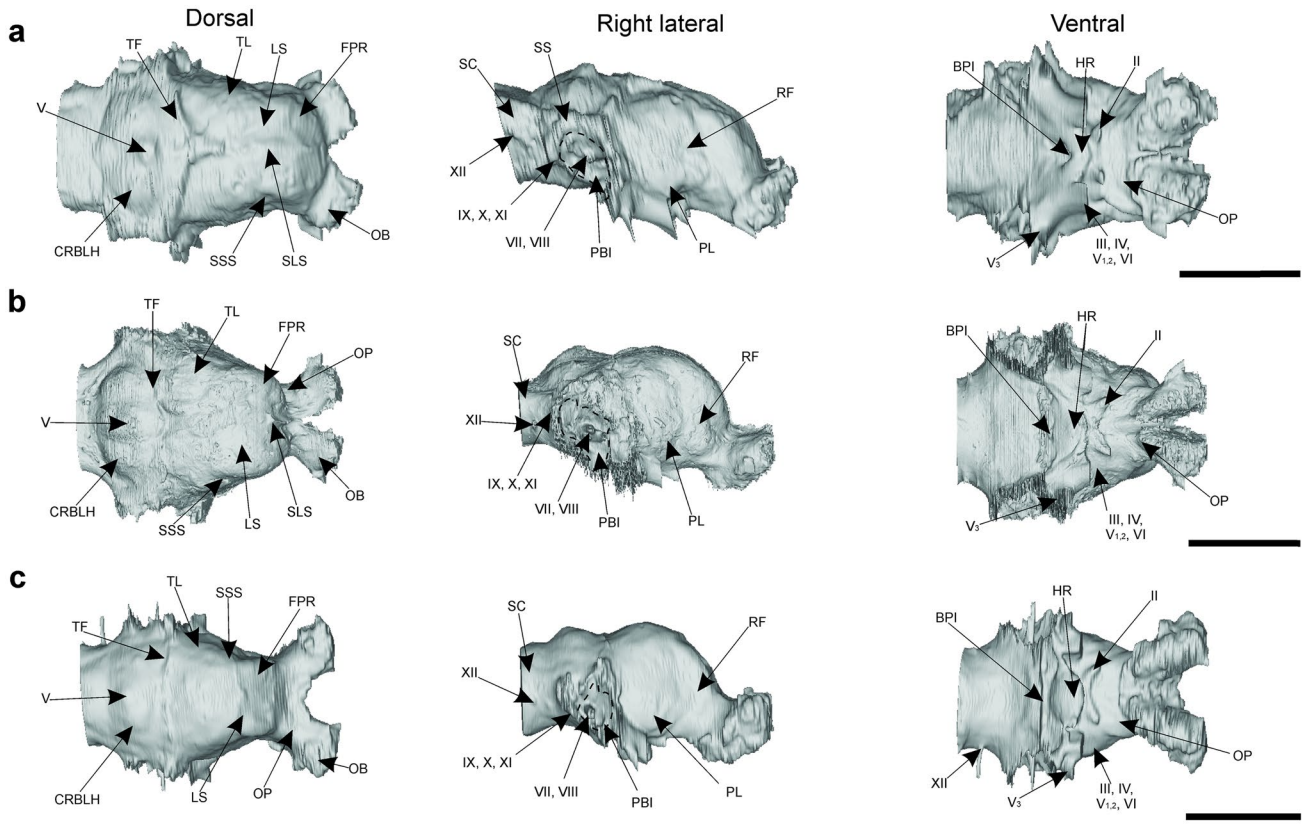

Fig. 4 Endocasts of Glyptodontoidea. **a**. *Doedicurus* sp. (MACN-Pv 2762); **b.** *Glyptodon* sp. (MNHN.F.PAM 759); **c.** *Panochthus tuberculatus* (MLP 16–38). Abbreviations: **BPI**, basilar process imprint; **CRBLH**, cerebellar hemispheres; **FPR**, frontoparietal region; **HR**, hypophyseal region; **LS**, lateral sulcus; **OB**, olfactory bulbs; **OP**, olfactory peduncules; **OTC**, orbito temporal canal; **PBI**, petrosal bone imprint; **PL**, piriform lobe; **PLP**, petrosal lobe of paraflocculus; **PRFCL**, parafocculus; **RCV**, rhinal caudal vein; **RF**, rhinal fissure; **SC**, spinal cord; **SLS**, superior longitudinal sinus; **SOTC**, sulci of ossified tentorium cerebelli; **SSS**, suprasylvian sulcus; **TF**, transverse fissure; **TL**, temporal lobe; **TS**, transverse sinus; **SS**, sigmoid sinus. The cranial nerves are indicated by roman numbers (II-XII). Scale bars equal 50 mm

the impression of a vestigial or a partially preserved ossified tentorium cerebelli.

Propalaehoplophorus shows a cerebellum that is slightly mediolaterally wider than the cerebral hemispheres, and the cerebellar hemispheres appear more mediolaterally expanded than the vermis in dorsal view (Fig. 3a). Besides, the cerebellum of *Propalaehoplophorus* is moderately extended anteroposteriorly, as in *Pampatherium* and *Holmesina* (Fig. 5; Tambusso and Fariña 2015b: fig. 2; Tambusso et al. 2023: fig. 4a, b) and in *Pseudoplohophorus* (Tambusso and Fariña 2015a: fig. 2). By contrast, extant armadillos show a more anteroposteriorly compressed cerebellum in dorsal view that also appears inflected ventrally in its anterior portion in lateral view (Fig. 6). On the contrary, Pleistocene glyptodonts show the greatest anteroposterior extension of the cerebellum in lateral view (Fig. 4).

The petrosal bone imprint is located ventrolaterally to the cerebellum and displays a convex semicircular margin, anteriorly and dorsally. The posterior depression related to the petrosal subarcuate fossa allows to identify a less differentiated petrosal lobule of the paraflocculus. This structure is dorsoventrally elongated and occupies almost the entire lateral cerebellar surface (Fig. 3b). This shape of the petrosal bone imprint is present in all glyptodonts (Fig. 4), pampatheres (Fig. 5b; Tambusso et al. 2023: fig. 4a, b), and *Chlamyphorus* (Fig. 6), whereas the remaining armadillos display a triangular contour in lateral view (Fig. 6). A detached petrosal lobe of the paraflocculus is not observable in Pleistocene glyptodonts (Fig. 4), but armadillos show a varying degree of development of this structure. In *Dasypus* and *Chlamyphorus*, the petrosal lobule is less developed than in hairy armadillos (Fig. 6). Regarding the posterior rhombencephalon, the spinal cord of *Pr. australis* is oriented ventrally as in *Ps. absolutus* (Tambusso and Fariña 2015a: fig. 2), pampatheres, and armadillos (Figs. 3, 4, 5 and 6; Tambusso et al. 2023: fig. 4a, b) but differs from the remaining glyptodonts, which show a spinal cord oriented parallel to the anteroposterior axis (Fig. 4). The pattern of blood vessels associated with the hindbrain is similar among cingulates. The sigmoid sinus leaves from the transverse sinus,

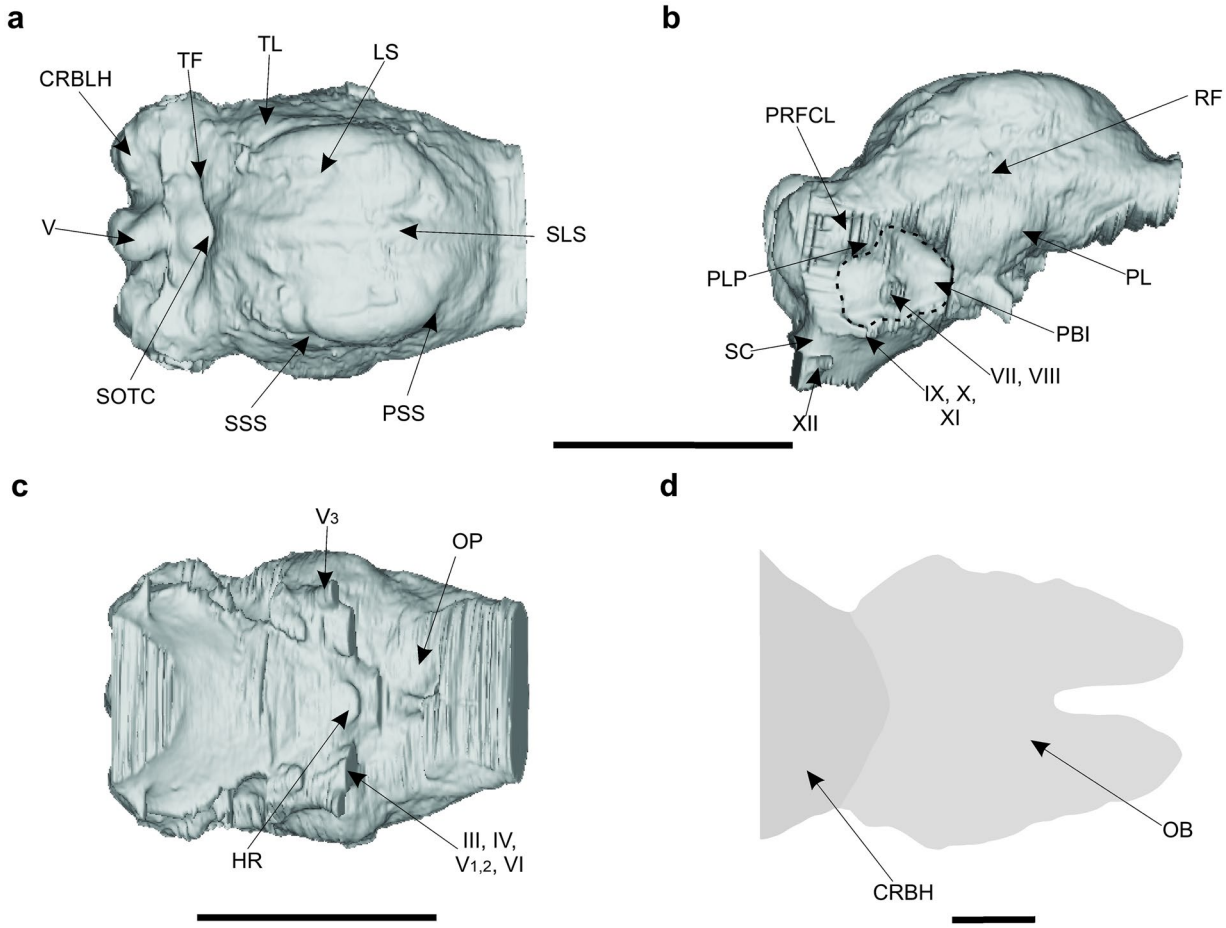

Fig. 5 Endocast of *Pampatherium typum* (MCAN-Pv 11543) in dorsal (**a**), right lateral (**b**), and ventral (**c**) views; **d**. detail of the olfactory bulbs of *P. humboldtii* in dorsal view, modified from Tambusso and Fariña (2015b). Abbreviations: **CRBH**, cerebral hemispheres; **CRBLH**, cerebellar hemispheres; **FPR**, frontoparietal region; **HR**, hypophyseal region; **LS**, lateral sulcus; **OB**, olfactory bulbs; **OP**, olfactory peduncules; **OTC**, orbito temporal canal; **PBI**, petrosal bone imprint; **PL**, piriform lobe; **PLP**, petrosal lobe of paraflocculus; **PRFCL**, parafocculus; **PSS**, presylvian sulcus; **RCV**, rhinal caudal vein; **RF**, rhinal fissure; **SC**, spinal cord; **SLS**, superior longitudinal sinus; **SOTC**, sulci of ossified tentorium cerebelli; **SSS**, suprasylvian sulcus; cerebelli; **TF**, transverse fissure; **TL**, temporal lobe; **TS**, transverse sinus. The cranial nerves are indicated by roman numbers (II-XII). Scale bars equal 50 mm in **a-c** and 10 mm in **d**

runs obliquely on the cerebellum, and crosses the cerebellar hemisphere above the paraflocculus to leave the skull through the jugular foramen (Figs. 3, 4, 5 and 6; Tambusso and Fariña 2015a: fig. 2).

Cranial nerves

In *Pr. australis* the olfactory surface of olfactory bulbs (CN I) is extended anteroventrally, displaying inclination respect to the anteroposterior axis of the skull (Fig. 3b). Ventrally, the roots of CNs II-XII are distinguishable (Fig. 3c). Immediately posterior to the last portion of the olfactory peduncles, the CN II diverges anteriorly and laterally. Posteriorly and medially to the root of CN II (optic chiasm), the cast of the confluent sphenorbital fissure and foramen rotundum (pierced by CNs III, IV, $V_{1\text{-}2,}$ and VI) shows a peculiar mediolaterally inflected pathway. By contrast, the root of CN V_3 is less evident. The mandibular branch of the trigeminal nerve leaves the skull without passing through a deep osseous canal, emerging on the cranial surface at the level of the foramen ovale. The facial (VII) and vestibulocochlear (VIII) nerves are more clearly distinguishable and cross the auditive internal meatus at the middle of the petrosal bone imprint. Cranial nerves IX, X, and XI emerge from the jugular foramen together with the sigmoid sinus, whereas the hypoglossal nerve (XII) is the only CN leaving the skull through the hypoglossal foramen (Fig. 3b).

Except for *Chlamyphorus*, which displays projections of CN I at the orthogonal plane to the anteroposterior axis, all cingulates here analyzed show an anteroventral extension of CN I (Figs. 3, 4, 5 and 6). The CN II diverges laterally in all the observed cingulates: *Dasypus*, *Chlamyphorus*,

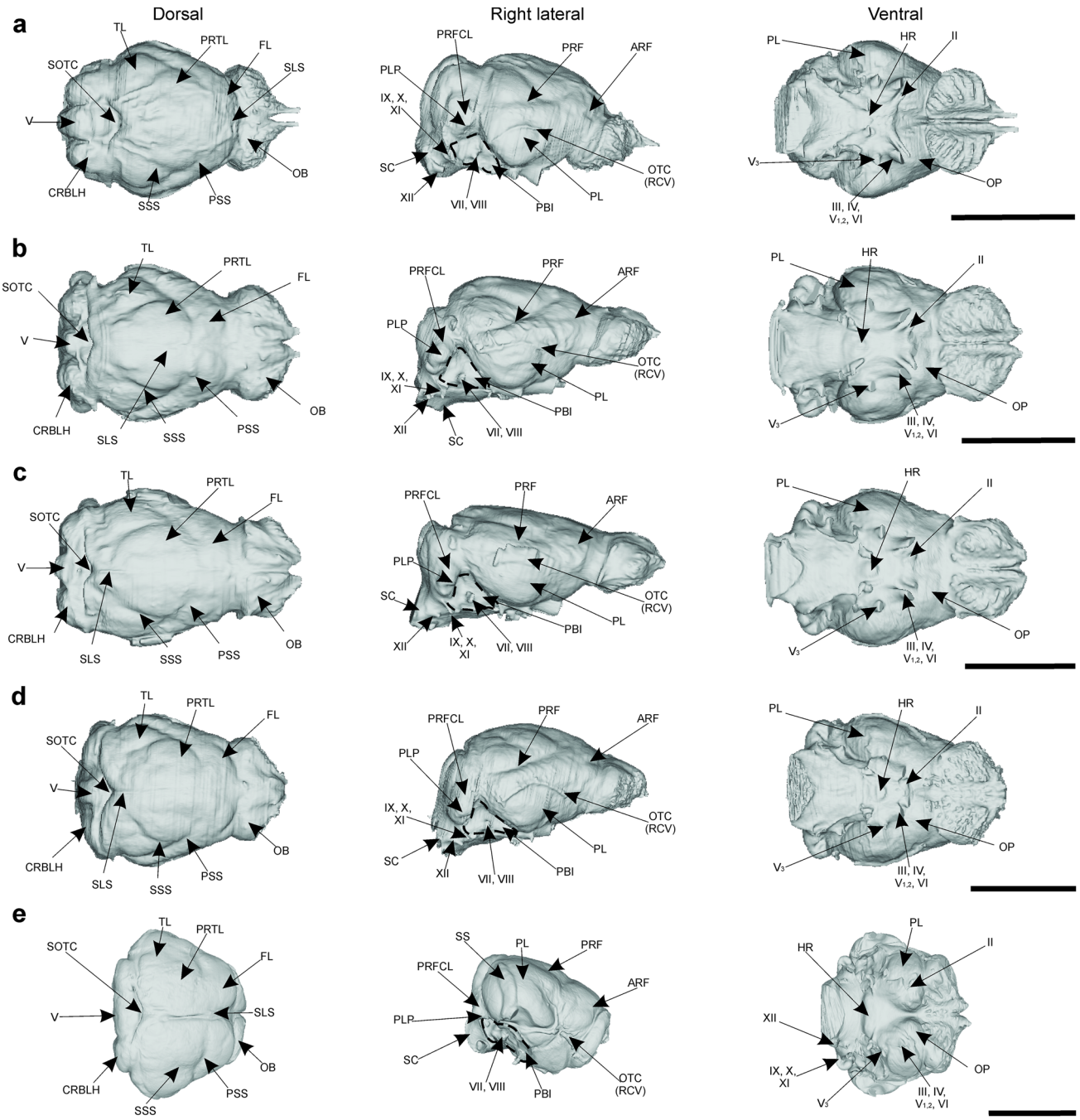

Fig. 6 Endocasts of armadillos. **a**. *Dasypus novemcinctus* (MACN-Ma 50.123); **b.** *Chaetophractus villosus* (MACN-Ma 27802); **c.** *Euphractus sexcinctus* (MACN-Ma 49.38); **d.** *Zaedyus pichyi* (MACN-Ma 30.33); **e.** *Chlamyphorus truncatus* (FMNH M 39468). Abbreviations: **ARF**, anterior rhinal fissure; **CRBLH**, cerebellar hemispheres; **FL**, frontal lobe; **HR**, hypophyseal region; **OB**, olfactory bulbs; **OP**, olfactory peduncules; **OTC**, orbito temporal canal; **PBI**, petrosal bone imprint; **PL**, piriform lobe; **PLP**, petrosal lobe of paraflocculus; **PRF**, posterior rhinal fissure **PRFCL**, parafloccu-lus; **PRTL**, parietal lobe; **PSS**, presylvian sulcus; **RCV**, rhinal caudal vein; **SC**, spinal cord; **SLS**, superior longitudinal sinus; **SOTC**, sulci of ossified tentorium cerebelli; **SSS**, suprasylvian sulcus; **TF**, transversal fissure; **TL**, temporal lobe; **TS**, transverse sinus. The cranial nerves are indicated by roman numbers (II-XII). Scale bars equal 50 mm in **a**-**d** and 10 mm in **e**

Holmesina, and *Panochthus* show greater lateral divergence, whereas in *Pampatherium* these nerves are directed more anteriorly (Figs. 4, 5 and 6; Tambusso et al. 2023: fig. 4a, b). Concerning CNs III, IV, $V_{1-2,}$ and VI, pampatheres and remaining glyptodonts display similar topological arrangements to *Propalaehoplophorus* (Figs. 4 and 5; Tambusso

et al. 2023: fig. 4a, b). On the other hand, in armadillos, these CNs appear closer to CN II than observed in the remaining cingulates (Fig. 6). The posterior and lateral divergent position of the short pathways of V_3 are observable in all glyptodonts, contrary to armadillos and pampatheres which display relatively less laterally divergent V_3 than the other cingulates (Figs. 4, 5 and 6; Tambusso et al. 2023: fig. 4a, b). Regarding the CNs from the posterior cranial fossa, the pathway arrangements of CNs VII-IX are similar in all cingulates. On the other hand, in *Pr. australis*, *Ps. absolutus*, pampatheres, and armadillos, the emergence of CN XII is located ventral to that of CNs VII-IX. In Pleistocene glyptodonts, CN XII emerges dorsal to or at the same level as CNs VII-IX, in lateral view (Figs. 3, 4, 5 and 6; Tambusso and Fariña, 2015a: fig. 2; Tambusso et al. 2023: fig. 4a, b).

Discussion

In this contribution, we analyzed the first digital endocast of the basal glyptodont *Propalaehoplophorus australis*. The neuromorphological similarities and differences observed among *Pr. australis,* Late Miocene and Pleistocene glyptodonts, pampatheres, and extant armadillos allowed us to explore some possible phylogenetically informative characters. The traits that are common to all Glyptodontia and pampatheres include the uninterrupted rhinal fissure, the presence of a small piriform lobe, the marked dorsal expansion of the neocortical frontal region, the conspicuous sinus longitudinal superior thickness, and the presence of a well-marked lateral sulcus. All these features could be potential synapomorphies in concordance with previous studies that recovered glyptodonts and pampatheres constituting a monophyletic group (Engelmann 1985; Gaudin and Wible 2006; Fernicola 2008; Billet et al. 2011; Fernicola and Porpino 2012; Herrera et al. 2017; Fernicola et al. 2018). However, reconstruction (i.e., visibility) of sinus longitudinal superior is related to inter cerebral hemispheric space marked by a portion of dura mater (i.e., falx cerebri) (Macrini et al. 2007a). Thus, this feature could be related to the external exposure of this vessel and not necessarily to its size or thickness. On the other hand, Dozo (1989) observed the presence of a lateral sulcus in the armadillos *Chaetophractus*, *Euphractus*, *Scagliatatus, Epipeltephilus*, and the glyptodont *Propalaehoplophorus,* proposing that this sulcus is homologue to the "Z groove" observed in sloths. Tambusso et al. (2023) suggested that the oblique sulcus in *Holmesina* and *Glyptodon* could be a topological homologous of the lateral sulcus. At least in the extant armadillos included here, the lateral sulcus is not well marked, unlike all the analyzed glyptodonts and pampatheres.

Other characters observed in *Pr. australis*, such as the absence of a presylvian *sulcus* and the presence of an anteroposteriorly continuous rhinal fissure, were also reported by Dozo (1998) in the Eocene armadillo *Utaetus buccatus*. Tambusso and Fariña (2015a) suggested that this neocortical sulcation pattern could represent a brain morphology that is ancestral to armadillos and glyptodonts. However, recent phylogenetic studies have proposed a different arrangement of *U. buccatus* (Herrera et al. 2017; Ciancio et al. 2021), suggesting a possible convergence between *U. buccatus* and glyptodonts in the neocortical sulcation pattern. A strong anteroposterior divergence of the olfactory bulbs is observable only in *Propalaehoplophorus,* in the pampatheres *Holmesina* and *Pampatherium*, and the giant armadillo *Priodontes* (Tambusso et al. 2023). These similarities could either represent a convergence among these genera or a synapomorphy shared by Pampatheriidae + Glyptodontia plus the basal Tolypeutinae *Priodontes* in concordance with phylogenetic hypotheses based on molecular data (Delsuc et al. 2016; Mitchell et al. 2016). Moreover, the longitudinal extension of sinus longitudinal superior shared by Miocene glyptodonts and *Priodontes* (Tambusso and Fariña 2015a; Tambusso et al. 2023) could support the close relationship between glyptodonts and tolypeutins. However, an anteroposterior secondary reduction of the olfactory bulbs would have occurred at the base of Glyptodontoinei, and an increase of divergence would have occurred in Glyptodontoidea (Fig. 2). *Propalaehoplophorus* shares exclusively with Glyptodontoinei the undivided frontoparietal lobes due to the absence of presylvian sulci and short and laterally directed CN V_3. These traits could represent synapomorphies of Glyptodontia. By contrast, other features, such as the undifferentiated petrosal lobule of the paraflocculus, the spinal cord oriented parallel to the anteroposterior axis, and the topological arrangement of CN XII, would represent potential synapomorphies of Glyptodontoidea (Fig. 2). The morphological variation of the anterior forebrain (i.e., olfactory bulbs and peduncles), could reflect an evolutionary constraint related to the topological arrangement described above. However, the anterior extension of olfactory peduncles observed in larger Glyptodontoidea (including the peculiar genus *Neosclerocalyptus*) could be related to a greater development of the paranasal sinuses (Christen et al. 2023 and references therein). In turn, this pneumatization could lighten the skull to avoid the biomechanical restrictions associated with telescoping of masticatory apparatus that increase skull inertia. Then, olfactory bulbs could potentially constrain internal skull morphological architecture in larger Pleistocene glyptodonts.

Propalaehoplophorus shares exclusively with Glyptodontoinei the undivided frontoparietal lobes due to the absence of presylvian sulci and short and laterally directed CN V_3. These traits could represent synapomorphies of Glyptodontia. By contrast, other features, such as the undifferentiated petrosal lobule of the paraflocculus, the spinal cord oriented parallel to the anteroposterior

axis, and the topological arrangement of CN XII, would represent potential synapomorphies of Glyptodontoidea (Fig. 2).

Concerning the dorsal separation between forebrain and hindbrain, Tambusso and Fariña (2015a, b) and Tambusso et al. (2023) suggested the presence of an ossified tentorium cerebelli in *Pampatherium humboldtii, Holmesina*, and extant armadillos, and its absence in glyptodonts, based on the presence/absence of an impression on the endocast. Our data confirm this hypothesis, as we observed a detached tentorium cerebelli in *Pampatherium typum* (MACN-Pv 11543), which leaves a deep sulcus on the dorsal surface of the brain endocast (Fig. 5). A similar but more reduced process is present in *Propalaehoplophorus,* right at the separation between the forebrain and the hindbrain, producing a step-like morphology on the dorsal surface of the brain endocast. This could represent either a vestigial or a poorly preserved tentorium cerebelli. In any case, further data is needed to evaluate the presence of a tentorium cerebelli in basal glyptodonts, a feature that is almost certainly lost in Glyptodontoidea (Tambusso and Fariña 2015a, b).

Among Cingulata, only Glyptodontoidea show a spinal cord that is mediolaterally wide in dorsal view and posterodorsally oriented in lateral view. This morphology could be related to their large body size (Vizcaíno et al. 2011a, 2012) and the consequent biomechanical demands of graviportality in head posture (Fariña and Vizcaíno 2001; Vizcaíno et al. 2004, 2011a), principally related to the tendency to collapse downward due to head bending moment, so crucial in mammals because of the extensive development of masticatory muscles (Arnold 2021). This trait could be increased in large Pleistocene glyptodonts due to the telescoping of masticatory apparatus added to greater development of craniomandibular muzzles than Miocene glyptodonts as *Propalaehoplophorus* (Vizcaíno et al. 2011a, b) or *Pseudoplohophorus* (Tambusso and Fariña 2015a; Tambusso et al. 2023).

Another feature that is likely linked with feeding strategies is the dorsal expansion of the cerebral anterior region, particularly evident in glyptodonts and pampatheres. This area has been tentatively related to specialized herbivory in open environments because a similar condition occurs in ungulates (Tambusso et al. 2023, and references therein). Previous ecomorphological studies based on body mass, relative masticatory muzzle width, hypsodonty index, and dental occlusal surface area have revealed that glyptodonts include dietary variation from selective to bulk feeding in relatively closed and open environments, respectively, while pampatheres displayed differential masticatory efficacy to coarse vegetal processing (Vizcaíno 2009; Vizcaíno et al. 2011b).

The petrosal lobule of the cerebellar paraflocculus (PLP) is probably linked with coordination, balance, and vestibular sensory perception (Macrini 2006), integrating visual, vestibular stimulus, and extraocular control muscles (Gannon et al. 1988; Ferreira-Cardoso et al. 2017). Extant megamammals (e.g., hippopotamids, proboscideans, and rhinoceroses) do not show distinct fossa subarquata in the petrosal bone, where the paraflocular lobe is located (Gannon et al. 1988; O'Leary 2010). Among the analyzed specimens, Pleistocene glyptodonts (above 800 kg) display an undifferentiated petrosal lobe of the paraflocculus, whereas extinct and extant smaller to large-sized cingulates (up to 210 kg) (Fariña et al., 1998; Vizcaíno et al. 2006, 2011a, 2012; Tambusso and Fariña 2015b) show a evident development of this structure, therefore suggesting a negative relationship of this feature with body size. Nevertheless, the giant ground sloth *Glossotherium* (ca. 1100 kg; Vizcaíno et al. 2006) display a distinguished parafloccular area, in contrast to small-sized extant relatives (i.e., less than 10 kg; *Bradypus* and *Choloepus*; Vizcaíno et al. 2006) which show a poorly development of this structure (Boscaini et al. 2018, 2020a). However, Ferreira-Cardoso et al. (2017) did not recover a direct relationship between the size of the paraflocculus and ecological/behavioral features and body mass, although xenarthrans and other large-sized mammals were not included in the analysis.

Tambusso et al. (2023) found strong similarities in the semicircular canals of the bony labyrinth, between glyptodonts and *Chlamyphorus,* and between Chlamyphoridae and pampatheres (*Holmesina*). Depending on the considered features, their results are alternatively congruent with molecular and morphological-based phylogenetic studies (Gaudin and Wible 2006; Billet et al. 2011; Delsuc et al. 2016; Mitchell et al. 2016; Herrera et al. 2017; Fernicola et al. 2018). In our sample, the anteroposteriorly elongated shape of the petrosal bone imprint on the brain endocast is shared by glyptodonts, pampatheres, and *Chlamyphorus*. This grouping is in concordance with the results of Tambusso et al. (2023) on the morphology of the semicircular canals, supporting the inclusion of glyptodonts and *Chlamyphorus* into Chlamyphoridae (Delsuc et al. 2016; Mitchell et al., 2016). Le Verger et al. (2021) found a close relationship between *Chlamyphorus* and glyptodonts, similar to Tambusso et al. (2023); however, in the former study, pampatheres (*Vassallia*) appear more related to glyptodonts than *Chlamyphorus*.

Conclusions

The brain morphology of *Propalaehoplophorus australis* shows strong morphological divergence from the Glyptodontei analyzed here, supporting its relatively basal position among Glyptodontia. In this latter group, *Propalaehoplophorus* displays more similarities, principally in the olfactory bulbs and the cerebellar region, with the moderate-sized *Pseudoplohophorus* and pampatheres than the larger Pleistocene glyptodonts. The similarities shared by

Propalaehoplophorus, *Pseudoplohophorus*, pampatheres, and *Priodontes* include the partial lateral divergence of the olfactory bulbs, the thickness of the superior longitudinal sulcus, and the marked anteroposterior compactness of the cerebellum in dorsal view. These similarities are probably indicative of phylogenetic relationships, but the effect of body size needs to be considered and properly evaluated.

When compared to other cingulates, the cerebellar region of *Propalaehoplophorus* is similar to that of the extant armadillos, whereas the anatomy of the auditive-vestibular region resembles that of *Chlamyphorus*. In this way, the present data support the idea that glyptodonts may represent a peculiar group of armadillos, as suggested by recent phylogenetic studies. In this way, the stronger similarities between *Propalaehoplophorus* and *Chlamyphorus* than other extant armadillos are congruent with the phylogenetic scenarios based on internal anatomy and molecular data. In general, the anatomy of the brain cavity appears as a promising field to investigate previously unobserved morphologies in a phylogenetic framework and contribute to the knowledge of the evolutionary history of glyptodonts and their relatives.

Supplementary information The online version contains supplementary material available at https://doi.org/10.1007/s10914-023-09689-x.

Acknowledgements We are grateful to the personnel of CEUNIM and, in particular, to Amalia Perez, Alejandro Valda, and collaborators for assistance with CT scans. We thank Marcelo Reguero (MLP), Pablo Teta (MACNMa), and Laura Chornogubsky and Laura Cruz (MACN-Pv), who kindly gave access to the specimens under their care. This work was possible thanks to the facilities offered by the free digitals database available at https://www.digimorph.org (National Science Foundation Dissertation Improvement Grant (EB-0309369) to Timothy Rowe and Thomas E. Macrini) and https://www.morphosource.org (OVert Project: oVert TCN, NSF DBI1702421; MNHN digital repository: curator of mammals in Paleontology in Paris (Guillaume Billet, CR2P), Marta Bellato of the AST-RX platform who made the acquisition, and Kevin Le Verger for share micro-CT data). We also want to thank Laura Montaldo and Denise Campos for their language revision, and finally to the Editor in Chief Darin Croft, and the anonymous reviewers whose comments and corrections greatly enhanced this manuscript. This work was funded by Agencia Nacional de Promoción Científica y Tecnológica (ANPyCT, FONCyT), PICT-2016-2665 PICT-2019-3551, PICT-2021-I-A-00271, and Universidad Nacional de Luján (UNLu) CDD-CB 013/19, 14/B293 and CDD-CB 086/20, PI4 2020 to AT.

Authors' contributions AT, GHC, AB, and JCF wrote the main manuscript text, GT made the microCT of MACN-Ma specimens, AT segmented the tomographies and prepared figures and tables. All authors reviewed the manuscript.

Funding This work was funded by Agencia Nacional de Promoción Científica y Tecnológica (ANPyCT, FONCyT), PICT-2016–2665 PICT-2019–3551, PICT-2021-I-A-00271, and Universidad Nacional de Luján (UNLu) CDD-CB 013/19, 14/B293 and CDD-CB 086/20, PI4 2020 to AT.

Availability of data and materials The complete dataset is available from AT upon request.

Declarations

Competing interests The authors declare no competing interests.

References

Abba AM, Cassini GH, Galliari FC (2011) Nuevos aportes a la historia natural de la mulita pampeana *Dasypus hybridus* (Mammalia, Dasypodidae). Iheringia Ser Zool 101:325–335. https://doi.org/10.1590/s0073-47212011000300007

Abba AM, Zufiaurre E, Codesido M, Bilenca DN (2015) Burrowing activity by armadillos in agroecosystems of central Argentina: Biogeography, land use, and rainfall effects. Agr Ecosyst Environ 200:54–61. https://doi.org/10.1016/j.agee.2014.11.001

Ahrens HE (2014) Morphometric study of phylogenetic and ecologic signals in procyonid (Mammalia: Carnivora) endocasts. Anat Record 297:2318–2330. https://doi.org/10.1002/AR.22996

Araújo JVS, Cavalcante MMA de S, Gonçalves PC de J, Guerra SPL, Da Silva ABS, Conde Júnior AM (2015) Descriptive macroscopic anatomy of the central nervous system six-banded armadillo (*Euphractus sexcintus*, Linnaeus, 1758) and nine-banded armadillo (*Dasypus novemcinctus*, Linnaeus, 1758). J Interdiscipl Biosci 1:13–17. https://doi.org/10.26694/2448-0002.vl1iss1pp13-17

Arnold P (2021) Evolution of the mammalian neck from developmental, morpho-functional, and paleontological perspectives. J Mamm Evol 28:173–183. https://doi.org/10.1007/s10914-020-09506-9

Aurboonyawat T, Pereira V, Kring T, Toulgoat F, Churojana A, Lasjaunias P (2008) Patterns of the cranial venous system from the comparative anatomy in vertebrates Part II The lateral-ventral venous system. Interv Neuroradiol 14:21–31. https://doi.org/10.1177/159101990801400103

Barasoain D, Zurita AE., Croft DA, Montalvo CI, Contreras VH, Miño-Boilini ÁR, Tomassini RL (2022) A New Glyptodont (Xenarthra: Cingulata) from the Late Miocene of Argentina: new clues about the oldest extra-patagonian radiation in southern South America. J Mamm Evol 29:263–282

Barnosky AD, Lindsey EL, Villavicencio NA, Bostelmann E, Hadly EA, Wanket J, Marshall CR (2016) Variable impact of Late-Quaternary megafaunal extinction in causing ecological state shifts in North and South America. Proc Natl Acad Sci USA 113:856–861.

Bertrand OC, San Martin-Flores G, Silcox MT (2019) Endocranial shape variation in the squirrel-related clade and their fossil relatives using 3D geometric morphometrics: contributions of locomotion and phylogeny to brain shape. J Zool 308:197–211. https://doi.org/10.1111/JZO.12665

Bertrand OC, Püschel HP, Schwab JA, Silcox MT, Brusatte SL (2021) The impact of locomotion on the brain evolution of squirrels and close relatives. Commun Biol 460.

Bertrand OC, Jiménez Lao M, Shelley SL, Wible JR, Williamson TE, Meng J, Brusatte SL (2023) The virtual brain endocast of *Trogosus* (Mammalia, Tillodontia) and its relevance in understanding the extinction of archaic placental mammals. J Anat. https://doi.org/10.1111/joa.13951

Billet, G, Hautier L, de Muizon C, Valentin X (2011) Oldest cingulate skulls provide congruence between morphological and molecular scenarios of armadillo evolution. Proc R Soc B 278:2791–2797. https://doi.org/10.1098/rspb.2010.2443

Billet G, Hautier L, Lebrun R (2015) Morphological diversity of the bony labyrinth (Inner Ear) in extant xenarthrans and its relation to phylogeny. J Mammal 96:658–672. https://doi.org/10.1093/jmammal/gyv074

Boscaini A, Iurino DA, Billet G, Hautier L, Sardella R, Tirao G, Gaudin TJ, Pujos F (2018) Phylogenetic and functional implications of the ear region anatomy of *Glossotherium robustum* (Xenarthra, Mylodontidae) from the Late Pleistocene of Argentina. Sci Nat 105:28. https://doi.org/10.1007/s00114-018-1548-y

Boscaini A, Iurino DA, Mamani Quispe B, Andrade Flores R, Sardella R, Pujos F, Gaudin TJ (2020a) Cranial anatomy and paleoneurology of the extinct sloth *Catonyx tarijensis* (Xenarthra, Mylodontidae) from the Late Pleistocene of Oruro, Southwestern Bolivia. Front Ecol Evol 8:69. https://doi.org/10.3389/fevo.2020.00069

Boscaini A, Iurino DA, Sardella R, Tirao G, Gaudin TJ, Pujos F (2020b) Digital cranial endocasts of the extinct sloth *Glossotherium robustum* (Xenarthra, Mylodontidae) from the Late Pleistocene of Argentina: description and comparison with the extant sloths. J Mamm Evol 27:55–71. https://doi.org/10.1007/s10914-018-9441-1

Carter TS, Superina M, Leslie DM (2016) *Priodontes maximus* (Cingulata: Chlamyphoridae). Mamm Species 48(932):21–34. https://doi.org/10.1093/mspecies/sew002

Cassini GH, Vizcaíno SF, Bargo MS (2012) Body mass estimation in Early Miocene native South American ungulates: A predictive equation based on 3D landmarks. J Zool 287:53–64. https://doi.org/10.1111/J.1469-7998.2011.00886.X

Christen ZM, Sánchez-Villagra MR, Le Verger K (2023). Cranial and endocranial comparative anatomy of the Pleistocene glyptodonts from the Santiago Roth Collection. Swiss J Palaeontol 142:1-32.

Ciancio MR, Vieytes EC, Castro MC, Carlini AA (2021) Dental enamel structure in long-nosed armadillos (Xenarthra: *Dasypus*) and its evolutionary implications. Zool J Linn Soc Lond 192:1237–1252. https://doi.org/10.1093/zoolinnean/zlaa119

Cignoni P, Callieri M, Corsini M, Dellepiane M, Ganovelli F, Ranzuglia G (2008) MeshLab: An open-source mesh processing tool. Proceedings of the Sixth Eurographics Italian Chapter Conference, pp 129–136

Cope ED (1889) The Edentata of North America. Am Nat 23:657–664

Croft DA, Flynn JJ, Wyss AR (2007) A new basal glyptodontid and other Xenarthra of the early Miocene Chucal Fauna, Northern Chile. J Vert Paleon 27:781–797. https://doi.org/10.1671/0272-4634(2007)27[781:ANBGAO]2.0.CO;2

Cuadrelli F, Zurita AE, Toriño P, Miño-Boilini ÁR, Perea D, Luna CA, Gillette DD, Medina O (2020) A new species of glyptodontine (Mammalia, Xenarthra, Glyptodontidae) from the Quaternary of the Eastern Cordillera, Bolivia: phylogeny and palaeobiogeography. J Syst Palaeontol 18:1543–1566. https://doi.org/10.1080/14772019.2020.1784300

Dechaseaux C (1958) Encéphales de xenarthres fossiles. In: Piveteau, J (ed) Traité de Paléontologie, Masson et Cie, París, pp 637–640

Dechaseaux C (1962) Encéfalos de notongulados y de desdentados xenarthros fósiles. Ameghiniana 2:193–209

De Iuliis G, Bargo MS, Vizcaíno SF (2001) Variation in skull morphology and mastication in the fossil giant armadillos *Pampatherium* spp. and allied genera (Mammalia: Xenarthra: Pampatheriidae), with comments on their systematics and distribution. J Vertebr Paleontol 20:743–754. https://doi.org/10.1671/0272-4634(2000)020[0743:VISMAM]2.0.CO;2

De Iuliis G, Pulerà D (2019) The Dissection of Vertebrates. Academic Press, Cambridge

Delsuc F, Stanhope MJ, Douzery EJP (2003) Molecular systematics of armadillos (Xenarthra, Dasypodidae): Contribution of maximum likelihood and Bayesian analyses of mitochondrial and nuclear genes. Mol Phylogenet Evol 28:261–275. https://doi.org/10.1016/S1055-7903(03)00111-8

Delsuc F, Gibb GC, Kuch M, Billet G, Hautier L, Southon J, Rouillard JM, Fernicola JC, Vizcaíno SF, MacPhee RDE, Poinar HN (2016) The phylogenetic affinities of the extinct glyptodonts. Curr Biol 26:155–156. https://doi.org/10.1016/j.cub.2016.01.039

Dozo MT (1987) The endocranial cast of an Early Miocene edentate, *Hapalops indifferens* Ameghino (Mammalia, Edentata, Tardigrada, Megatheriidae): Comparative study with brains of recent sloths. J Hirnforsc 28:397–406

Dozo MT (1989) Estudios correlativos paleo-neoneurológicos en edentados xenartros (Mammalia, Edentata, Xenarthra): neuroevolución. Dissertation, Universidad Nacional de La Plata, Argentina

Dozo MT (1994) Interpretación del molde endocraneano de *Eucholoeops fronto*, un Megalonychidae (Mammalia, Xenarthra, Tardigrada) del Mioceno temprano de Patagonia (Argentina). Ameghiniana 31:317–329

Dozo MT (1998) Neuromorfología de *Utaetus buccatus* (Xenarthra, Dasypodidae): un armadillo del Eoceno temprano de la Provincia del Chubut, Argentina. Ameghiniana 35:285–289.

Dozo MT, Martínez G (2016) First digital cranial endocasts of late Oligocene Notohippidae (Notoungulata): Implications for endemic South American ungulates brain evolution. J Mamm Evol 23:1–16. https://doi.org/10.1007/s10914-015-9298-5

Engelmann GF (1985) The phylogeny of the Xenarthra. In: G.G. Montgomery (ed) The Evolution and Ecology of Armadillos, Sloths and Vermilinguas, Smithsonian Institution Press, Washington, D.C., pp 51–64

Fariña RA, Vizcaíno SF (2001) Carved teeth and strange jaws: How glyptodonts masticated. Acta Palaeontol Pol 46:219–234

Fariña RA, Vizcaíno SF, Bargo MS (1998) Body mass estimations in Lujanian (Late Pleistocene-Early Holocene of South America) mammal megafauna. Mastozool Neotrop 5:87–108

Fedorov A, Beichel R et al (2012) 3D Slicer as an image computing platform for the Quantitative Imaging Network. Magn Reson Imaging 30:1323–1341. https://doi.org/10.1016/J.MRI.2012.05.001

Fernández-Monescillo M, Antoine PO, Pujo, F, Gomes Rodrigues H, Mamani Quispe B, Orliac M (2019) Virtual endocast morphology of Mesotheriidae (Mammalia, Notoungulata, Typotheria): New insights and implications on notoungulate encephalization and brain evolution. J Mamm Evol 26:85–100. https://doi.org/10.1007/s10914-017-9416-7

Fernicola JC (2008) Nuevos aportes para la sistemática de los Glyptodontia Ameghino 1889 (Mammalia, Xenarthra, Cingulata). Ameghiniana 45:553–574

Fernicola JC, Porpino KO (2012) Exoskeleton and systematics: A historical problem in the classification of glyptodonts. J Mamm Evol 19:171–183. https://doi.org/10.1007/s10914-012-9186-1

Fernicola JC, Toledo N, Bargo MS, Vizcaíno SF (2012) A neomorphic ossification of the nasal cartilages and the structure of paranasal sinus system of the glyptodont *Neosclerocalyptus* Paula Couto 1957 (Mammalia, Xenarthra). Palaeontol Electron 15:1–22. https://doi.org/10.26879/333

Fernicola JC, Rinderknecht A, Jones W, Vizcaíno SF, Porpino K (2018) A new species of *Neoglyptatelus* (Mammalia, Xenarthra, Cingulata) from the Late Miocene of Uruguay provides new insights on the evolution of the dorsal armor in cingulates. Ameghiniana 55:233–252. https://doi.org/10.5710/AMGH.02.12.2017.3150

Fernicola JC, Zimicz AN, Chornogubsky L, Ducea M, Cruz LE, Bond M, Arnal M, Cárdenas M, Fernández M (2021) The Early Eocene climatic optimum at the lower section of the Lumbrera Formation (Ypresian, Salta province, Northwestern Argentina): origin and early diversification of the Cingulata. J Mamm Evol 28:621–633. https://doi.org/10.1007/S10914-021-09545-W

Ferreira-Cardoso S, Araújo R, et al (2017) Floccular fossa size is not a reliable proxy of ecology and behaviour in vertebrates. Sci Rep 7:2005. https://doi.org/10.1038/s41598-017-01981-0

Gallo JA, Fasola L, Abba AM (2019) Armadillos as natural pests control? Food habits of five armadillo species in Argentina. Mastozool Neotrop 26:117–127. https://doi.org/10.31687/saremMN.19.26.1.0.03

Gannon PJ, Eden AR, Laitman JT (1988) The subarcuate fossa and cerebellum of extant primates: Comparative study of a skull-brain interface. Am J Phys Anthropol 77:143–164. https://doi.org/10.1002/ajpa.1330770202

Gaudin TJ, Wible JR, (2006) The phylogeny of living and extinct armadillos (Mammalia, Xenarthra, Cingulata): a craniodental analysis.

In: Carrano MT, Gaudin TJ, Blob RW, Wible JR (eds) Amniote Paleobiology: Perspectives on the Evolution of Mammals, Birds, and Reptiles. University of Chicago Press, Chicago, pp 153–198

Gaudin TJ, Mcdonald HG (2008) Morphology-based investigations of the phylogenetic relationships among extant and fossil xenarthrans. In: Vizcaíno SF, Loughry WJ (eds) The Biology of the Xenarthra. University Press of Florida, Florida, pp 24–36

Gaudin TJ, Croft DA (2015) Paleogene Xenarthra and the evolution of South American mammals. J Mammal 96:622–634. https://doi.org/10.1093/jmammal/gyv073

Gervais P (1869) Mémoire sur les formes cérébrales propres aux édentés vivants et fossiles. Nouv Arch Mus Hist Nat Paris 5:1–56

Gibb GC, Condamine, FL, Kuch M, Enk J, Moraes-Barros N, Superina M, Poinar, HN, Delsuc, F (2016) Shotgun mitogenomics provides a reference phylogenetic framework and timescale for living xenarthrans. Mol Biol Evol 33:621–642. https://doi.org/10.1093/molbev/msv250

Gillette DD, Ray CE (1981) Glyptodonts of North America. Smithson Contrib Paleobiol 40:1–255. https://doi.org/10.5479/SI.00810266.40.1

Herrera CMR, Powell JE, Esteban GI, del Papa C (2017) A new Eocene dasypodid with caniniforms (Mammalia, Xenarthra, Cingulata) from Northwest Argentina. J Mamm Evol 24:275–288. https://doi.org/10.1007/s10914-016-9345-x

Huxley TH (1865) II. On the osteology of the genus *Glyptodon*. Philos Trans R Soc Lond 155:31–70. https://doi.org/10.1098/RSTL.1865.0002

Le Verger K, González Ruiz L R, Billet G (2021) Comparative anatomy and phylogenetic contribution of intracranial osseous canals and cavities in armadillos and glyptodonts (Xenarthra, Cingulata). J Anat 239(6):1473–1502. https://doi.org/10.1111/joa.13512

Lydekker R (1894) Contribuciones al conocimiento de los vertebrados fósiles de la Argentina. Part II. An Mus La Plata 2:1–248

Machado FA, Marroig G, Hubbe A (2022) The pre-eminent role of directional selection in generating extreme morphological change in glyptodonts (Cingulata; Xenarthra). Proc R Soc B 289:20212521. https://doi.org/10.1098/rspb.2021.2521

McKenna MC, Bell SK (1997) Classification of Mammals Above the Species Level. Columbia University Press, New York

Macrini TE (2006) The evolution of endocranial space in mammals and non-mammalian cynodonts. Dissertation, The University of Texas

Macrini TE, Rougier GW, Rowe T (2007a) Description of a cranial endocast from the fossil mammal *Vincelestes neuquenianus* (Theriiformes) and its relevance to the evolution of endocranial characters in therians. Anat Record 290:875–892. https://doi.org/10.1002/ar.20551

Macrini TE, Rowe T, Vandenberg JL (2007b) Cranial endocasts from a growth series of *Monodelphis domestica* (Didelphidae, Marsupialia): A study of individual and ontogenetic variation. J Morphol 268:844–865. https://doi.org/10.1002/JMOR.10556

Macrini TE, Flynn JJ, Croft DA, Wyss AR (2010) Inner ear of a notoungulate placental mammal: anatomical description and examination of potentially phylogenetically informative characters. J Anat 216:600–610.

Martínez, G, Dozo MT, Vera B, Cerdeño E (2019) Paleoneurology, auditory region, and associated soft tissue inference in the late Oligocene notoungulates *Mendozahippus fierensis* and *Gualta cuyana* (Toxodontia) from central-western Argentina. J Vertebr Paleontol 39:1–19. https://doi.org/10.1080/02724634.2019.1725531

Mitchell KJ, Scanferla A, Soibelzon E, Bonini R, Ochoa J, Cooper A (2016) Ancient DNA from the extinct South American giant glyptodont *Doedicurus* sp. (Xenarthra: Glyptodontidae) reveals that glyptodonts evolved from Eocene armadillos. Mol Ecol 25:3499–3508. https://doi.org/10.1111/MEC.13695

Núñez Blasco A, Zurita AE;, Miño Boilini AR, Bonini RA, Cuadrelli F (2021) The glyptodont *Eleutherocercus solidus* from the late Neogene of north-western Argentina: Morphology, chronology, and phylogeny. Acta Palaeontol Pol 66:79–99.

O'Leary MA (2010) An anatomical and phylogenetic study of the osteology of the petrosal of extant and extinct artiodactylans (Mammalia) and relatives. Bull Am Mus Nat Hist 335:1–206. https://doi.org/10.1206/335.1

O'Leary MA, Bloch JI et al (2013) The placental mammal ancestor and the post–K-Pg radiation of placentals. Science 339:662–667. https://doi.org/10.1126/science.1229237

Orliac MJ, O'Leary MA (2016) The inner ear of *Protungulatum* (Pan-Euungulata, Mammalia). J Mamm Evol 23:337–352. https://doi.org/10.1007/s10914-016-9327-z

Orliac MJ, Argot C, Gilissen E (2012) Digital cranial endocast of *Hyopsodus* (Mammalia, "Condylarthra"): a case of Paleogene terrestrial echolocation? PLoS One 7:e30000. https://doi.org/10.1371/journal.pone.0030000

Owen-Smith RN (1988) Megaherbivores: the Influence of Very Large Body Size on Ecology. Cambridge University Press, Cambridge

Padberg J (2017) Xenarthran nervous systems. In: Kaas JH, (ed) Evolution of Nervous Systems, 2nd Ed, vol. 2. Academic Press, Nashville, pp 383–412

Perini FA, Macrini TE, Flynn JJ, Bamba K, Ni X, Croft DA, Wyss AR (2022) Comparative endocranial anatomy, encephalization, and phylogeny of Notoungulata (Placentalia, Mammalia). J Mamm Evol 29:369–394 https://doi.org/10.1007/s10914-021-09583-4

Porpino KDO, Fernicola JC, Bergqvist LP (2010) Revisiting the intertropical brazilian species *Hoplophorus euphractus* (Cingulata, Glyptodontoidea) and the phylogenetic affinities of *Hoplophorus*. J Vertebr Paleontol 30:911–927. https://doi.org/10.1080/02724631003765735

Porpino KDO, Fernicola JC, Cruz LE, Bergqvist LP (2014) The intertropical Brazilian species of *Panochthus* (Xenarthra, Cingulata, Glyptodontoidea): A reappraisal of their taxonomy and phylogenetic affinities. J Vertebr Paleontol 34:1165–1179 https://doi.org/10.1080/02724634.2014.863203

Prates L, Perez SI (2021) Late Pleistocene South American megafaunal extinctions associated with rise of Fishtail points and human population. Nat Commun 12:2175.

Prothero DR (2017) Xenarthra, sloths, anteaters, and armadillos. In: The Princeton Field Guide to Prehistoric Mammals. Princeton University Press, New Jersey, pp 51–57. https://doi.org/10.1515/9781400884452

Quiñones SI, Miño-Boilini ÁR, Zurita AE, Contreras SA, Luna CA, Candela AM, Camacho M, Ercoli MD, Solís N, Brandoni D (2019) New records of Neogene Xenarthra (Mammalia) from eastern Puna (Argentina): diversity and biochronology. J Paleontol 93:1258–1275. https://doi.org/10.1017/jpa.2019.64

Superina M (2011) Husbandry of a pink fairy armadillo (*Chlamyphorus truncatus*): Case study of a cryptic and little known species in captivity. Zoo Biol 30:225–231. https://doi.org/10.1002/zoo.20334

Tambusso PS, Fariña RA (2015a) Digital cranial endocast of *Pseudoplohophorus absolutus* (Xenarthra, Cingulata) and its systematic and evolutionary implications. J Vertebr Paleontol 35:e967853. https://doi.org/10.1080/02724634.2015.967853

Tambusso P, Fariña RA (2015b) Digital endocranial cast of *Pampatherium humboldtii* (Xenarthra, Cingulata) from the Late Pleistocene of Uruguay. Swiss J Palaeontol 134:109–116. https://doi.org/10.1007/s13358-015-0070-5

Tambusso PS, Varela L, Góis F, Moura JF, Villa C, Fariña RA (2021) The inner ear anatomy of glyptodonts and pampatheres (Xenarthra, Cingulata): Functional and phylogenetic implications. J S Am Earth Sci 108:103189. https://doi.org/10.1016/j.jsames.2021.103189

Tambusso PS, Góis F, Moura JF, Villa C, do Amaral RV (2023) Paleoneurology of extinct cingulates and insights into their inner ear anatomy. In: Dozo MT, Paulina-Carabajal A, Macrini TE, Walsh S (eds) Paleoneurology of Amniotes. Springer, Cham, Switzerland pp 711–736. https://doi.org/10.1007/978-3-031-13983-3_18

Treuting PM, Dintzis S, Montine KS (2017) Comparative Anatomy and Histology: a Mouse, Rat, and Human Atlas. Academic Press, Cambridge

Vizcaíno SF (2009) The teeth of the "toothless": novelties and key innovations in the evolution of xenarthrans (Mammalia, Xenarthra). Paleobiology 35:343–366. https://doi.org/10.1666/0094-8373-35.3.343

Vizcaíno SF, De Iuliis G, Bargo MS (1998) Skull shape, masticatory apparatus, and diet of *Vassallia* and *Holmesina* (Mammalia: Xenarthra: Pampatheriidae): when anatomy constrains destiny. J Mamm Evol 5:291–322. https://doi.org/10.1023/A:1020500127041

Vizcaíno SF, Farina RA, Bargo MS, De Iuliis G (2004) Functional and phylogenetic assessment of the masticatory adaptations in Cingulata (Mammalia, Xenarthra). Ameghiniana 41:651–664

Vizcaíno SF, Bargo MS, Cassini GH (2006) Dental occlusal surface area in relation to body mass, food habits and other biological features in fossil xenarthrans. Ameghiniana 43:11–26

Vizcaíno SF, Blanco RE, Bender JB, Milne N (2011a) Proportions and function of the limbs of glyptodonts. Lethaia 44:93–101. https://doi.org/10.1111/j.1502-3931.2010.00228.x

Vizcaíno SF, Cassini GH, Fernicola JC, Bargo MS (2011b) Evaluating habitats and feeding habits through ecomorphological features in glyptodonts (Mammalia, Xenarthra). Ameghiniana 48:305–319 https://doi.org/10.5710/AMGH.v48i3(364)

Vizcaíno SF, Fernicola JC, Bargo MS (2012) Paleobiology of Santacrucian glyptodonts and armadillos (Xenarthra, Cingulata). In: Vizcaíno SF, Kay RF, Bargo MS (eds) Early Miocene Paleobiology in Patagonia: High-Latitude Paleocommunities of the Santa Cruz Formation. Cambridge University Press, Cambridge, pp 194–215

Wallace RB and Painter RLE (2013) Observations on the diet of the giant armadillo (Priodontes maximus Kerr, 1792). Edentata 14:85–86.

Witmer LM, Ridgely RC (2008) The paranasal air sinuses of predatory and armored dinosaurs (Archosauria: Theropoda and Ankylosauria) and their contribution to cephalic structure. Anat Record 291:1362–1388. https://doi.org/10.1002/ar.20794

Zurita AE, González Ruiz LR, Gómez-Cruz AJ, Arenas-Mosquera JE (2013a) The most complete known Neogene Glyptodontidae (Mammalia, Xenarthra, Cingulata) from northern South America: Taxonomic, paleobiogeographic, and phylogenetic implications. J Vertebr Paleontol 33:696–708. https://doi.org/10.1080/02724634.2013.726677

Zurita AE, Taglioretti M, Zamorano M, Scillato-Yané GJ, Luna C, Boh D, Saffer MM (2013b) A new species of *Neosclerocalyptus* Paula Couto (Mammalia: Xenarthra: Cingulata): The oldest record of the genus and morphological and phylogenetic aspects. Zootaxa 3721:387–398. https://doi.org/10.11646/zootaxa.3721.4.6

Zurita AE, Scillato-Yané GJ, Ciancio M, Ruiz (2016a) Los Glyptodontidae (Mammalia, Xenarthra): Historia biogeográfica y evolutiva de un grupo particular de mamíferos acorazados. Contrib Cient Mus Arg Cienc Nat "Bernardino Rivadavia" 6:249–262

Zurita AE, Taglioretti M, de los Reyes M, Cuadrelli F, Poire D (2016b) Regarding the real diversity of Glyptodontidae (Mammalia, Xenarthra) in the late Pliocene (Chapadmalalan Age/Stage) of Argentina. An Acad Bras Cienc 88:809–827. https://doi.org/10.1590/0001-3765201620150113